Struct Multidisc Optim (2006) 31: 251–259
DOI 10.1007/s00158-005-0584-3

RESEARCH PAPER

A. Gersborg-Hansen · M. P. Bendsøe · O. Sigmund

Topology optimization of heat conduction problems using the finite volume method

Received: 3 August 2005 / Revised manuscript received: 28 September 2005 / Published online: 2 March 2006

Abstract This note addresses the use of the finite volume method (FVM) for topology optimization of a heat conduction problem. Issues pertaining to the proper choice of cost functions, sensitivity analysis, and example test problems are used to illustrate the effect of applying the FVM as an analysis tool for design optimization. This involves an application of the FVM to problems with nonhomogeneous material distributions, and the arithmetic and harmonic averages have here been used to provide a unique value for the conductivity at element boundaries. It is observed that when using the harmonic average, checkerboards do not form during the topology optimization process.

Keywords Topology optimization · Heat conduction · Finite volume method · Sensitivity analysis

1 Introduction

This note considers the solution of a prototype topology optimization problem using the finite volume method (FVM) for solving the underlying physical problem. The work is motivated by the fact that the FVM is a mature technology widely used in engineering practice and the existence of advanced finite volume solvers used in the fluid mechanics community (Chalot 2004; Vos et al. 2002). Here we consider a heat diffusion problem to demonstrate the basic technicalities of solving a topology optimization problem involving the use of the FVM (see also Sigmund 2001b,c; Donoso and Sigmund 2004; Diaz and Benard 2003; Bendsøe and Sigmund 2004; Li et al. 2004; Habbal et al. 2004 for advanced examples involving heat conduction). This allows us to illustrate the basic difficulties of implementing topology design using the FVM that uses finite difference approximations in the formulation of the state problem.

In transport problems, a possible new area of application for topology optimization, the FVM is a relevant numerical scheme (see Jenny et al. 2004) since it guarantees element-wise conservation of the fundamental physical quantities, as described in Barth and Ohlberger (2004). Conservation of mass is very critical in reactive flows since it is related to the well-posedness of the mathematical model; as already noted, FVM is a standard analysis method for fluid problems.

We note that optimization of fluid dynamic problems is a well-established research field, but the application of topology optimization to fluid problems is quite new, cf., Mohammadi and Pironneau (2004). Borrvall and Petersson (2003) investigated topology optimization of Stokes flow problems to design energy-efficient fluid devices, and topology optimization of fluid network problems was considered by Klarbring et al. (2003). Recently, the concept of a topological derivative has also been introduced by Guillaume and Idris (2005), as a new tool for shape optimization. The seminal work Borrvall and Petersson (2003) has been extended to include the effect of inertia in Sigmund et al. (2003), Evgrafov (2004), Gersborg-Hansen et al. (2005a), and Olesen et al. (2005), and new work on topology optimization of transport problems was presented in Thellner (2005). Following the tradition in the structural optimization community, these papers share the use of the finite element method (FEM) for solving the underlying physical problem, hindering users of FVM easy access to the topology optimization tool.

The optimization of heat conduction problems follows here the standard lines of topology design by a material distribution technique. Based on the heat conduction concept, this paper also briefly introduces an idea of extending topology optimization for layout optimization in civil engineering problems that could be a theme pursued in future research. The works of Bejan (2000) and Bejan and Ledezma (1998) introduce the idea of considering the flow of heat from a volume to a single point as a way of attacking the minimization of travel time in an urban area. Other inspiration can be obtained from Craig et al. (2001), who use mathematical programming techniques for an urban geometry to

Preliminary results of the work reported here were presented at the WCSMO 6 in Rio de Janeiro 2005, see Gersborg-Hansen et al. (2005b).

A. Gersborg-Hansen (✉) · M. P. Bendsøe
Department of Mathematics, Technical University of Denmark, 2800, Lyngby, Denmark
e-mail: agh@mek.dtu.dk

O. Sigmund
Department of Mechanical Engineering, Solid Mechanics, Technical University of Denmark, 2800, Lyngby, Denmark

minimize pollution, from Jha and Schonfeld (2004), who consider highway shape optimization using geographic information systems, from Jong and Schonfeld (2003), who employ genetic algorithms to optimize 3D highway alignment in a rural area, and from Bartholdi and Gue (2004), who consider the optimal shape of a transit plant.

2 FVM for heat conduction

We follow here the textbook by Versteeg and Malalasekera (1995) in setting up the FVM equations.

Let $\Omega \subset \mathbb{R}^2$ be a spatial design domain with boundary $\Gamma = \overline{\Gamma_\mathrm{D} \cup \Gamma_\mathrm{N}}$, $\Gamma_\mathrm{D} \cap \Gamma_\mathrm{N} = \emptyset$ partitioned in a Dirichlet (D) and a Neumann (N) part. On Ω, we consider the steady-state heat equation given in its strong form and with homogeneous boundary conditions

$$\nabla \cdot (k \nabla T) + f = 0 \text{ in } \Omega \tag{1a}$$

$$T = 0 \text{ on } \Gamma_\mathrm{D} \tag{1b}$$

$$(k \nabla T) \cdot \mathbf{n} = 0 \text{ on } \Gamma_\mathrm{N} \tag{1c}$$

where T is the temperature, k the heat conduction coefficient, f the volumetric heat source, and $\mathbf{n}$ an outward unit normal vector. Moreover, the heat flux is defined as $\mathbf{q} = k \nabla T$. The physical meaning of the boundary conditions is that the temperature at Γ_D is fixed at $T = 0$ and the boundary Γ_N is insulated (adiabatic).

With topology optimization in mind, we consider a state field (temperature) and a design field (conductivity) on Ω. The discrete representation of the two fields is seen in Fig. 1 and is based on nodal values. Two regular grids are used, one for each field. In the following section, a topology optimization problem is formulated such that an optimal conduction field $k = k(\mathbf{x})$ is determined using topology optimization; see Bendsøe and Sigmund (2004).

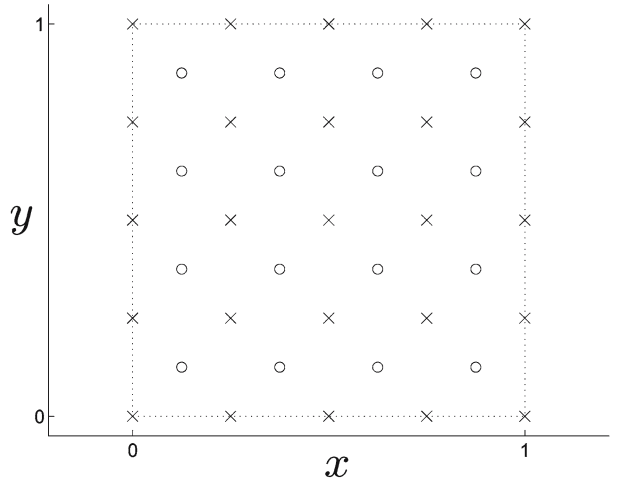

Fig. 1 Spatial domain with state nodes '×', design nodes 'o', and physical boundary '···'

The FVM form of the heat equation is obtained by integrating over subdomains Ω_e and formally applying the Gauss theorem:

$$\int_{\Omega e} (\nabla \cdot (k \nabla T) + f) = 0 \tag{2a}$$

$$\Rightarrow \quad \int_{\partial \Omega_e} (k \nabla T) \cdot \mathbf{n} + \int_{\Omega_e} f = 0 \quad \forall_e \tag{2b}$$

where $\mathbf{n}$ is a unit normal vector.

For the discretization at hand (cf., Fig. 1), the FVM test volumes Ω_e are obtained by defining a surrounding volume for each node in the domain; see Fig. 2b. On each state volume, we require the governing FVM (2b) to be satisfied using a finite difference approximation for the temperature gradient. To calculate the heat flux at the element interface, some average value of the conductivity is used. Two averages have been tested

$$\langle k \rangle_{(\cdot)} \begin{cases} \dfrac{1}{n} \displaystyle\sum_{i=1}^{n} k_i & \text{(Voigt, arithmetric)} \\ n \left(\displaystyle\sum_{i=1}^{n} \frac{1}{k_i} \right)^{-1} & \text{(Reuss, harmonic)} \end{cases} \tag{3}$$

where k_i is a nodal value. For $n = 2$, we obtain an average across or along a face of the test volume, and with $n = 4$, we can obtain a volume average over the test volume. Note that in 1D heat conduction, the harmonic average gives the effective conductance at the interface, cf., Patankar (1980), and from a material mixtures' point of view, the arithmetic and harmonic averages correspond to the Voigt and Reuss bounds, respectively.

The FVM directly employs finite differences for the temperature gradients. For regular meshes, as typically used for topology optimization, this provides first-order accuracy of the heat flux at element boundaries. Volume integrals, such as the right-hand side of (2b), are defined as the average value over the element, cf., Versteeg and Malalasekera (1995). This corresponds to a linear interpolation over the element.

For a state element in the interior, (2b) is evaluated as

$$(\mathbf{q}_\mathtt{e} \cdot \mathbf{n}_\mathtt{e} + \mathbf{q}_\mathtt{w} \cdot \mathbf{n}_\mathtt{w}) h_y + (\mathbf{q}_\mathtt{n} \cdot \mathbf{n}_\mathtt{n} + \mathbf{q}_\mathtt{s} \cdot \mathbf{n}_\mathtt{s}) h_x + f h_x h_y = 0 \tag{4}$$

where h_x and h_y are the element width and height, respectively. $\mathbf{q}_{(\cdot)} \cdot \mathbf{n}_{(\cdot)}$ is the outward normal heat flux at the element faces $\{\mathtt{w}, \mathtt{e}, \mathtt{s}, \mathtt{n}\}$ (for west, east, south, north). The flux is evaluated using a first-order finite difference approximation, e.g., for the west side with respect to $T_{i,j}$

$$\mathbf{q}_\mathtt{w} \cdot \mathbf{n}_\mathtt{w} = \langle k \rangle_\mathtt{w} \frac{T_{i,j} - T_{i-1,j}}{\delta x} (-1) \tag{5}$$

with δx being the x-distance between two temperature nodes. In the present case, $\delta x = h_x$, cf., Fig. 2, except for boundary elements.

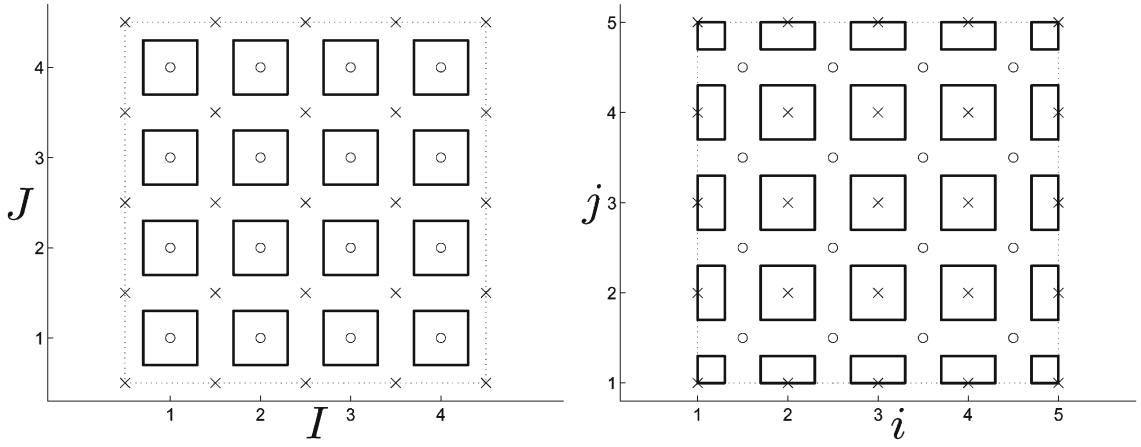

Fig. 2 Sketch of finite volume discretization used. Design variables (conductivity) are cell centered '∘' and form the primal mesh with coordinates (I, J). State variables (temperature) are '×' and form the dual mesh with coordinates (i, j). For clarity, the volumes are shown somewhat shrunken—in the implementation, they cover the domain completely. The physical boundary is represented by '· · · '

For the element with the state node $T_{i,j}$, we denote by $\tilde{\mathbf{u}}$ the vector that contains $T_{i,j}$ and the neighbors associated with a first-order finite difference approximation

$$\tilde{\mathbf{u}} = \left[T_{i-1,j}\, T_{i+1,j}\, T_{i,j-1}\, T_{i,j+1}\, T_{i,j}\right]^{\mathrm{T}} \tag{6}$$

with $(\cdot)^{\mathrm{T}}$ denoting the transpose operator. Then (4) for this element becomes

$$\left[-\xi_{\mathtt{w}} - \xi_{\mathtt{e}} - \xi_{\mathtt{s}} - \xi_{\mathtt{n}} \sum \xi\right] \tilde{\mathbf{u}}_i = f h_x h_y \tag{7}$$

where $\xi(\cdot)$ is evaluated at the element faces

$$\xi_{\mathtt{H}} = \frac{\langle k \rangle_{\mathtt{H}} h_y}{\delta_x},\ \xi_{\mathtt{V}} = \frac{\langle k \rangle_{\mathtt{v}} h_x}{\delta_y} \tag{8}$$

with $\mathtt{H} = \{\mathtt{w}, \mathtt{e}\}$, $\mathtt{V} = \{\mathtt{s}, \mathtt{n}\}$ and $\sum\xi$ being the sum of the face contributions in (8).

Neumann boundary conditions fit directly into the FVM framework. For Dirichlet boundary conditions, we here apply a penalty method, as suggested in Versteeg and Malalasekera (1995) and Patankar (1980).

Using a standard assembly procedure of the contribution (7), a matrix problem is obtained

$$\mathbf{K}\mathbf{u} = \mathbf{f} \tag{9}$$

where the matrix $\mathbf{K}$ is symmetric, $\mathbf{u}$ is the temperature vector, and $\mathbf{f}$ the thermal load vector. The two vectors both contain nodal values defined at the center of the state elements.

One drawback of the FVM is the way boundary conditions at $\partial\Omega$ are treated; the use of finite difference approximations complicates implementation. Also, the use of one-sided finite difference operators for elements at the boundary means that special attention is needed in the solution of the state problem, and for optimization, in the evaluation of the cost functions and in the associated sensitivity analysis. Here we only illustrate the implementation for the interior elements and describe the treatment of the boundary elements in Appendix 1.

3 Topology optimization

We consider here a generic topology optimization problem following Bendsøe and Sigmund (2004):

$$\begin{aligned} \min_{\mathbf{a}\in\mathbb{R}^m} \quad & c(\mathbf{a}) \\ \text{s.t.} \quad & \sum_{i=1}^{m} A_i a_i \le V^*,\ 0 < a_{\min} \le a_i \le a_{\max} \end{aligned} \tag{10}$$

Here a_i is a design variable, A_i element area, and $c(\mathbf{a})$ the cost function. The problem has a volume constraint in addition to the box constraints on the design variables ($a_{\min} = 10^{-3}$ and $a_{\max} = 1$), and the equilibrium equation $\mathbf{K}(\mathbf{a})\mathbf{u} = \mathbf{f}$ is assumed as the basis for evaluating $c(\mathbf{a})$. The conductivity $k = k(\mathbf{x})$ entering the matrix $\mathbf{K}$ is controlled by the design variables following a slightly modified solid isotropic material with penalization (SIMP) rule

$$\breve{\mathbf{k}} = \mathbf{s}(\mathbf{a}), \quad s_i(\mathbf{a}) = 10^{-3} + (1 - 10^{-3}) a_i^p \tag{11}$$

where $\breve{\mathbf{k}}$ is a vector with nodal conductivity values, and p is a penalty factor. The computational procedure used to solve (10) is in this work based on the use of the MMA algorithm; see Svanberg (1987, 2002). A continuation approach is adopted such that p is gradually increased to the final value $p = 3$ to obtain 0–1 designs (for details, see Bendsøe and Sigmund 2004).

3.1 Cost function

We consider here a cost function which is equivalent to compliance in structural problems. Physically, the optimization problem then corresponds to finding the conductivity distribution $k(\mathbf{x})$ that produces the least heat when the amount of high conduction material is limited, relevant to the design of

an optimal heat-conducting device. For the continuum setting, we have two equal expressions for the cost function:

$$c_{\mathrm{I}} = \int_{\Omega} fT \tag{12a}$$

$$c_{\mathrm{II}} = \int_{\Omega} \nabla T \cdot \mathbf{q} = \int_{\Omega} \nabla T \cdot (k \nabla T) \tag{12b}$$

where $\mathbf{q}$ is the heat flux vector. For an FEM discretization, we also have $c_{\mathrm{I}} = c_{\mathrm{II}}$, in agreement with the principle of virtual work. However, this is not the case for the finite volume analysis. For an FVM implementation, the use of c_{I} may be the natural choice (it does not involve derivatives). However, we here also consider c_{II}, as one may, in other optimization problems, encounter situations where gradient expressions occur, and it is thus relevant to understand how c_{II} can be handled in an FVM setting.

When using the FVM, there is not a unique way to evaluate integrals such as (12b), as the variables are only available at specific points. Thus, different FVM interpretations of c_{II} are available.

If we choose to treat the integrand in (12b) similarly to the source term of the state equation, one would apply straight averages. This gives a quadratic form in T:

$$c_{\mathrm{II}}^{q} = \sum_{\mathrm{ne}} \langle k \rangle_V (\nabla T \cdot \nabla T) A \tag{13}$$

where $\langle k \rangle_V$ is a volume average, and ne abbreviates 'number of elements'; choosing the arithmetic average corresponds to a linear interpolation of k over the element.

Alternatively, one can first rewrite c_{II} by applying the Green–Gauss theorem for (12b) and then use the strong form of (1a):

$$\begin{aligned} c_{\mathrm{II}} &= \sum_{\mathrm{ne}} \int_{\Omega_e} \nabla T \cdot \mathbf{q} \\ &= \sum_{\mathrm{ne}} \left\{ \int_{\partial \Omega_e} (T\mathbf{q}) \cdot \mathbf{n} + \int_{\Omega_e} fT \right\} \end{aligned} \tag{14}$$

where we now work with the normal heat flux across interfaces. This then can lead to the interpretation:

$$c_{\mathrm{II}}^{F} = \sum_{\mathrm{ne}} \left\{ \sum_{\mathrm{ef}} \left((\langle T \rangle^{a} \mathbf{q}) \cdot \mathbf{n} l \right) + fTA \right\} \tag{15}$$

in which one applies an arithmetic average for the temperature $\langle T \rangle^{a}$ across a face; also ef abbreviates 'number of element faces,' and l is the length of the face. For the FVM, the boundary contribution is zero because the flux is balanced and the average value $\langle T \rangle^{a}$ is the same across internal element boundaries, and thus, $c_{\mathrm{I}} = c_{\mathrm{II}}^{F}$. The average temperature is used because a continuous temperature field is expected from a physical point of view.

3.2 Sensitivity analysis

We use the adjoint method to derive the sensitivity $\frac{\mathrm{d}c}{\mathrm{d}a_i}$ needed by a gradient-driven optimization algorithm (cf., e.g., Choi and Kim 2005). The sensitivity analysis can be done analytically when using c_{I}, but for c_{II}, the solution of an adjoint problem is required.

We first streamline the notation by defining the finite difference operators using matrices

$$c_{\mathrm{II}}^{q} = \sum_{\mathrm{ne}} \tilde{\mathbf{u}}^{\mathrm{T}} \tilde{\boldsymbol{\mathcal{K}}} \tilde{\mathbf{u}} A \tag{16}$$

where $\tilde{\mathbf{u}}$ is given by (6). $\tilde{\boldsymbol{\mathcal{K}}}$ is symmetric and defined by

$$\tilde{\boldsymbol{\mathcal{K}}} = \langle k \rangle_V \mathbf{B}^{\mathrm{T}} \mathbf{B}, \quad \mathbf{B} = \begin{bmatrix} \frac{-1}{2h_x} & \frac{1}{2h_x} & 0 & 0 & 0 \\ 0 & 0 & \frac{-1}{2h_y} & \frac{1}{2h_y} & 0 \end{bmatrix} \tag{17}$$

where h_x and h_y are the element width and height, respectively.

Next, we write a Lagrangian in the form

$$\mathcal{L} = \mathbf{u}^{\mathrm{T}} \tilde{\mathbf{K}} \mathbf{u} + \boldsymbol{\lambda}^{\mathrm{T}} (\mathbf{K}\mathbf{u} - \mathbf{f}) \tag{18}$$

where $\tilde{\mathbf{K}}$ is an assembled version of (17), and $\mathbf{f}$ is independent of the design. This—by standard derivation—gives the sensitivity as

$$\frac{\mathrm{d}c}{\mathrm{d}a_i} = \frac{\mathrm{d}s_j}{\mathrm{d}a_i} \left(\mathbf{u}^{\mathrm{T}} \frac{\partial \tilde{\mathbf{K}}}{\partial s_j} + \boldsymbol{\lambda}^{\mathrm{T}} \frac{\partial \mathbf{K}}{\partial \mathrm{s_j}} \right) \mathbf{u} \tag{19}$$

where $\boldsymbol{\lambda}$ is the solution to the adjoint problem

$$\mathbf{K}^{\mathrm{T}} \boldsymbol{\lambda} = -\left(\tilde{\mathbf{K}} + \tilde{\mathbf{K}}^{\mathrm{T}} \right) \mathbf{u} \tag{20}$$

Since $\mathbf{K}$ is symmetric, the adjoint problem is efficiently solved using back substitution. Note that the cost function matrix $\tilde{\mathbf{K}}$ is not necessarily symmetric for some interpretations of c_{II}, but for c_{II}^{q}, it is symmetric. Also note that the result is somewhat different from what is typically seen for FEM, due to the fact that in FVM, the matrices $\mathbf{K}$ and $\tilde{\mathbf{K}}$ do not coincide.

The implementation of the above follows standard adjoint sensitivity analysis procedures with a slight deviation when calculating $\frac{\partial \mathbf{K}}{\partial s_i}$. As depicted in Fig. 3, each design variable enters in the system matrix $\mathbf{K}$ in four rows through the averages, cf., (7) and (8). Thus, we find

$$\frac{\partial \mathbf{K}}{\partial s_i} \mathbf{u} = \begin{bmatrix} {}^{1}\xi'_{\mathrm{e}} + {}^{1}\xi'_{\mathrm{n}} & -{}^{1}\xi'_{\mathrm{e}} & 0 & -{}^{1}\xi'_{\mathrm{n}} \\ -{}^{2}\xi'_{\mathrm{w}} & {}^{2}\xi'_{\mathrm{w}} + {}^{2}\xi'_{\mathrm{n}} & -{}^{2}\xi'_{\mathrm{n}} & 0 \\ 0 & -{}^{3}\xi'_{\mathrm{s}} & {}^{3}\xi'_{\mathrm{s}} + {}^{3}\xi'_{\mathrm{w}} & -{}^{3}\xi'_{\mathrm{w}} \\ -{}^{4}\xi'_{\mathrm{s}} & 0 & -{}^{4}\xi'_{\mathrm{e}} & {}^{4}\xi'_{\mathrm{s}} + {}^{4}\xi'_{\mathrm{e}} \end{bmatrix} \begin{bmatrix} {}^{1}u \\ {}^{2}u \\ {}^{3}u \\ {}^{4}u \end{bmatrix} \tag{21}$$

using the notation shown in Fig. 3. For the test examples presented below, the sensitivities were checked using a real and complex finite difference approximation. The complex variable trick is typically not applied in structural optimization problems but is a strong and valuable tool, cf., Squire and Trapp (1998) (see also van Keulen et al. 2005).

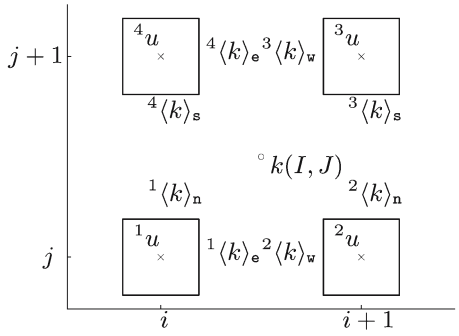

Fig. 3 Link between node $k(I, J)$ and the face conductivities $\langle k\rangle_{(\cdot)}$ at surrounding state elements. The state elements are numbered counterclockwise ${}^1u, \ldots, {}^4u$ to clarify the implementation

4 Test problems

Two types of test problems have been investigated. They differ by the types of boundary conditions that are considered for the reference domain Ω, which is the unit square in both cases. One problem has the total length of the west and north boundaries of Dirichlet type, cf., Fig. 4d, so that for a homogeneous layout, high regularity of the state is to be expected, and thus, FEM and FVM should be quantitatively similar in the limit of mesh refinement. The other problem has only a small part of the west boundary with a Dirichlet boundary condition, cf., Fig. 6d, so here low regularity is expected and the boundary condition is tricky to implement. Here, one sees that FVM and FEM behave differently even for the homogeneous case. However, the designs that are obtained are similar in nature.

The volumetric forcing is $f = 10^{-2}$ in both problems. The filter proposed by Sigmund (2001a) and Bendsøe and Sigmund (2004) that can control the formation of checkerboards and control geometry is used in some examples. Here, the filter radius is chosen so that only checkerboards are removed, and it does not impose geometry constraints on the design beyond the mesh scale (the filter is thus here mesh-dependent).

4.1 Case 1

Figure 4 shows the final designs for the minimization of the cost function c_I using a finite element approach and using the FVM with the arithmetic average ($\mathrm{FVM_a}$) as well as the harmonic average ($\mathrm{FVM_h}$). Using the $\mathrm{FVM_a}$ without filtering led to the same type of checkerboards that are well known from topology optimization using the FEM. The checkerboards can be removed by the filtering mentioned above or by using the harmonic average in the FVM formulation. The

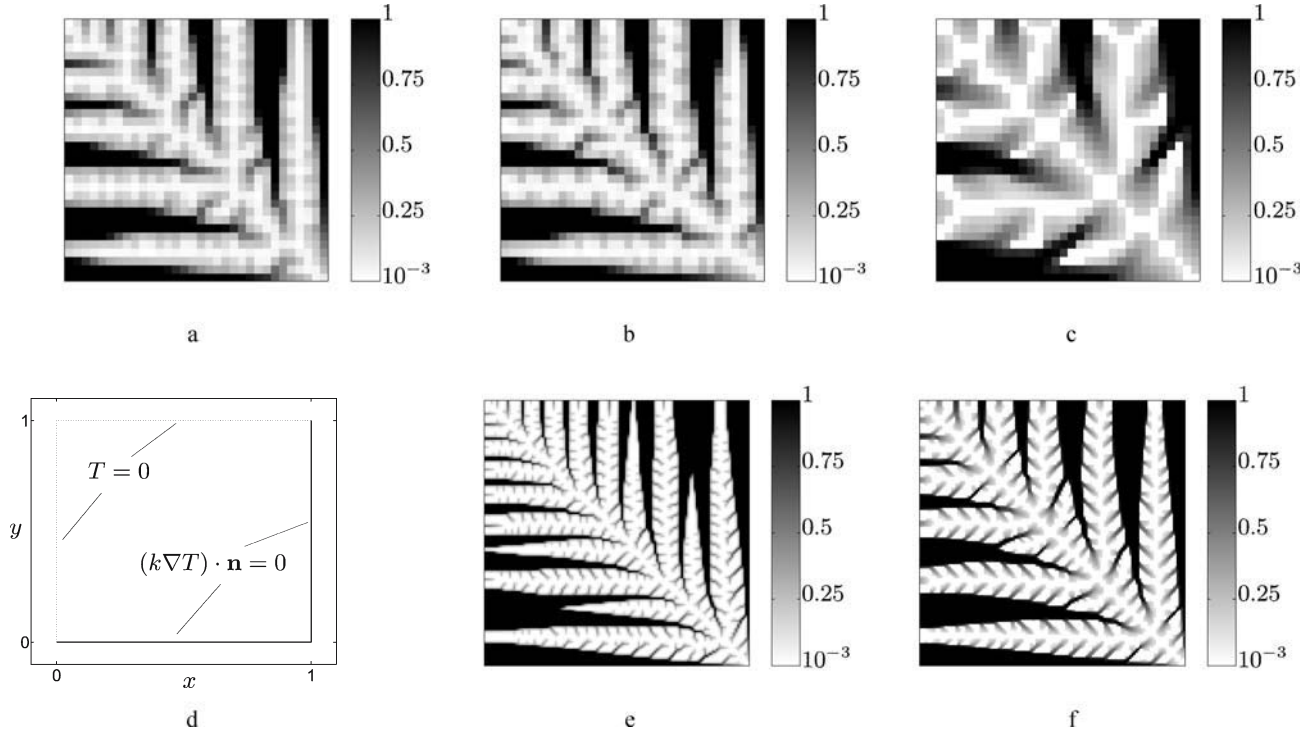

Fig. 4 Design examples with the cost function c_I with $V^* = 0.4$. Boundary conditions are seen in **d**. For the designs in **c** and **f**, no filter is used. The sensitivities have been filtered using the Sigmund filter (see Sigmund 2001a) for the designs in **a**, **b**, and **e**. **a** $\mathrm{FEM^f}$, with filter. 32×32 design variables, $c_\mathrm{I} = 5.10\times10^{-5}$. **b** $\mathrm{FVM_a^f}$ (arithmetic), with filter. 32×32 design variables, $c_\mathrm{I} = 4.97\times10^{-5}$. **c** $\mathrm{FVM_h}$ (harmonic), no filter. 32×32 design variables, $c_\mathrm{I} = 7.27\times10^{-5}$. **d** Boundary conditions. $T = 0$ on west and north side ($\cdots$) and $(k\nabla T)\cdot\mathbf{n} = 0$ on east and south side (—). **e** $\mathrm{FVM_a^f}$ (arithmetic), with filter. 128×128 variables, $c_\mathrm{I} = 3.82\times10^{-5}$. **f** $\mathrm{FVM_h}$ (harmonic), no filter. 128×128 design variables, $c_\mathrm{I} = 4.58\times10^{-5}$

designs obtained are qualitatively similar to results obtained by Donoso and Sigmund (2004) for pressurized membranes, which are also governed by the Poisson equation.

Using continuation and a final penalization value $p=5$ reduces the amount of intermediate densities, which appear using the harmonic average. In addition, computations show that constructing an average of the material properties being a linear combination of the arithmetic and harmonic average gives control of the amount of intermediate densities/checkerboards without filtering of the sensitivities.

Employing $\mathrm{FVM_h}$ yields results that are not 0–1 designs, and the cost function differs from the corresponding FEM and $\mathrm{FVM_a}$ results, cf., Fig. 4a–c. This can be explained by the use of the harmonic average that interpolates gray densities differently.

Note also that a substantial amount of gray is present in the $\mathrm{FVM_h}$ design. It is thus relevant to verify that the interpolation scheme (11) does not violate the well-known conduction materials so that a gray density would be realized as a composite material such a composite would then be constructed with a fraction a of a high conducting material (e.g., copper) and a fraction $(1-a)$ of a material with a negligible conduction (e.g., polystyrene).

Several authors have studied the physical realizability of intermediate densities in topology optimization problems that involve elasticity; see Bendsøe and Sigmund (1999), Stolpe and Svanberg (2001), Pedersen (2004). Performing the same calculation as in Bendsøe and Sigmund (1999) and using the upper Hashin–Shtrikman bounds for conduction—originally derived in Hashin and Shtrikman (1962) and shown for the 2D case in Hashin (1983) and Torquato et al. (1998)—one finds that for the ordinary SIMP interpolation $s_i^{\mathrm{SIMP}} = a_i^p$, $p \geq 2$ is a necessary and sufficient condition. For the slightly modified SIMP rule (11), the Hashin–Shtrikman bound is violated for very small densities. However, for a density $a_i > 3\times10^{-3}$, the bounds are met, and hence, for the range of densities that are shown as gray, one can interpret such areas as consisting of a composite.

Designs obtained using the cost function c_{II}^q are seen in Fig. 5. They are qualitatively similar to the designs obtained using the cost function c_{I}, cf., Fig. 4. However, computations done with 128×128 design variables indicate that the cost function c_{II}^q is strongly mesh dependent since the designs obtained suffer from intermediate densities, although the penalty factor is increased beyond $p=5$. Thus, the cost function c_{I} should be used.

4.2 Case 2

This problem has a solution that is less regular than the previous test problem since the change from the Dirichlet to the Neumann boundary condition does not happen at a corner, cf., Fig. 6d. The FEM framework is able to handle such an abrupt change in the boundary conditions, whereas the FVM which is based on the strong form has problems—this is evident from a convergence study of a uniform design (this discussion is beyond the scope of this work). In turn, this voids quantitative comparisons between the values of the cost functions for Fig. 6a–c. However, from a qualitative point of view, they are similar in nature. Analogous FEM results are presented in Donoso and Sigmund (2004) and Bendsøe and Sigmund (2004).

4.3 Possible future application

Figure 6e–f illustrates an idea of an application of topology optimization in urban planing tasks such as optimal traffic layout. One may also think that escape route layouts on music festivals and in large sports arenas would benefit from using topology optimization. The latter cases enjoy the property of being planar problems with constant population density similar to the volumetric heating used in this note.

5 Discussion

The present work demonstrates that topology optimization is possible in a finite volume setting, and that it requires minor deviations in the sensitivity analysis compared to a conventional finite element implementation.

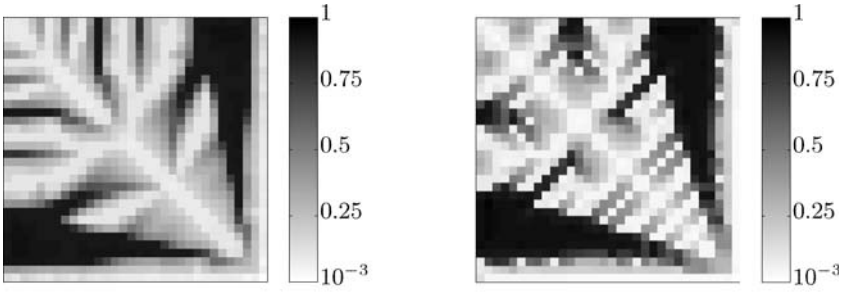

Fig. 5 Designs obtained for the cost function c_{II}^q. Design examples with 32×32 design variables, $V^* = 0.4$ and boundary conditions seen in Fig. 4d. **a** FEM_a^f (arithmetic), with filter. $c_{\mathrm{II}}^q = 7.12\times10^{-5}$. **b** $\mathrm{FVM_h}$ (harmonic), no filter. $c_{\mathrm{II}}^q = 6.25\times10^{-5}$

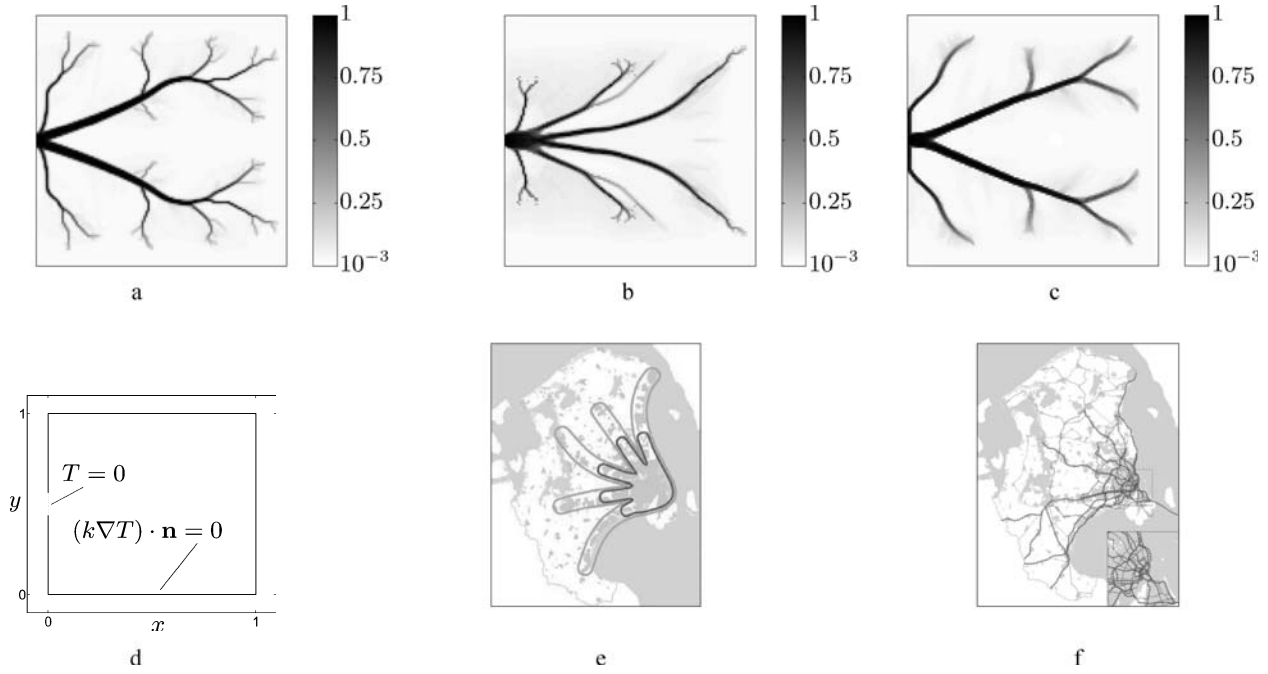

Fig. 6 Designs obtained for the cost function c_I measuring the nonregular temperature field caused by the boundary conditions seen in **d**. For **a–c**, 128×128 design variables are used, $V^* = 0.1$ and $\gamma = 1/128$. The difference in the way the FEM and the FVM handle the nonsmooth boundary conditions does not yield a qualitative difference in the design. **e–f** Description of common urban planning task which could be a future application of topology optimization. One may also think that escape route layouts on music festivals and in large sports arenas may benefit from using topology optimization. **a** FEM^{f}, with filter. $c_I = 1.30\times10^{-3}$. **b** $\text{FVM}^{\text{f}}_{\text{a}}$ (arithmetic), with filter. $c_I = 1.93\times10^{-3}$. **c** FVM_{h} (harmonic), no filter. $c_I = 1.65\times10^{-3}$. **d** Boundary conditions. $T = 0$ on a fraction γ of the west side $(\cdots)$ and $(k\nabla T) \cdot \mathbf{n} = 0$ on Γ_N (—). **e** The five-finger plan for traffic layout near Copenhagen: 'small hand' in the year 1947 and 'large hand' in the year 2003. From Hovedstadens Udviklingsråd (2003). **f** Implemented solution in the year 2003. From Hovedstadens Udviklingsråd (2003)

A number of topology optimization problems involving steady-state heat conduction have been solved on a staggered mesh using the arithmetic and harmonic average for interpolation between nodal values of material data. This is consistent with the FVM, and the averages correspond to the well-known Voigt and Reuss bounds. The use of the arithmetic average gives rise to the formation of checkerboards during the optimization process, but they can be avoided by the implementation of a sensitivity filter. However, when using the harmonic average, checkerboards do not form, and by combining the arithmetic and harmonic averages, one obtains control of the amount of checkerboards in the design without filtering of the sensitivities.

Boundary conditions are handled differently in the FVM compared to the FEM, in particular, in the case of lack of boundary regularity. One such problem is considered, and it appears that the difference does not play a qualitative role for the design.

We note that it is unfavorable from a theoretical point of view to use a flux-based method based on finite difference approximations in problems with jumps in the material parameters as typically seen in topology design. One can speculate that the optimization will exploit this, and that convergence of the discretized problems cannot be obtained, even in a regularized format. For future applications, it may thus be advantageous to consider the implementation of the Discontinuous Galerkin Method (Lesaint and Raviart 1974; Cockburn et al. 1999) since it is a higher order method with a direct link to the variational problem.

On the other hand, when using very mature FVM codes for optimization purposes such as transport-dominated flow problems, one may accept such theoretical disadvantages in engineering practice.

Acknowledgements This work received financial support from Denmark's Technical Research Council under the "Phonon project" grant number 26-02-0217. The authors are grateful for the helpful comments from the anonymous reviewers, which has improved the paper in several aspects. In addition, the authors thank Per Grove Thomsen, Christian Lotz Felter, Bjarne Skovmose Kallesøe, and Dalibor Cavar from Technical University of Denmark and Martin Berggren from Department of Information Technology, Division of Scientific Computing, Uppsala University for helpful discussions related to this work.

Appendix: Treatment of boundary contributions

This appendix briefly describes the implementation of boundary conditions in FVM, see the excellent reference Versteeg and Malalasekera (1995) for further details. For the planar problems considered, there are two types of boundary elements, namely, those at edges and those at corners. The properties h_x and h_y vary for the elements at the boundary, necessitating a number of loops when performing the assembly of the matrix $\mathbf{K}$. This should be compared to the single loop operation used for finite elements on structured grids frequently occurring in topology optimization, cf., e.g., Sigmund (2001a).

As mentioned in Section 2, we have used a penalty approach to enforce Dirichlet conditions. This effectively decouples the Dirichlet nodes from the rest of the system of equations by addition of a large scalar to the diagonal elements. Zero flux Neumann boundary conditions are enforced by letting the appropriate $\xi(\cdot)$ equal to zero and formally moving it to the right-hand side, cf., (7).

When it comes to the design field, an interior state node is surrounded by four design nodes, whereas a boundary state node is surrounded by two or one; see Fig. 2. In this work, we have made use of a strategy that copies the values of the design nodes for a boundary element in the direction of the outward normal to some fictitious design nodes. In this way, a corner element would have one design node and three fictitious design nodes, all with the same value, and an edge element would have two design nodes with fictitious copies at the same values. For the sensitivity analysis, this has the advantage that the procedure illustrated for an interior element in Fig. 3 applies also for the boundary nodes, provided that the fictitious state nodes are included. In turn, the Neumann boundary condition is satisfied by choosing the same nodal value on both sides of Γ_{N}.

The evaluation of the sensitivity of the cost function c_{I} is straightforward to implement, but for other interpretations such as c_{II}^{q}, it is more challenging, as the state and the design fields are here evaluated explicitly and refer to the two staggered grids.

References

Barth T, Ohlberger M (2004) Finite volume methods: foundation and analysis. In: Stein E, Borst R, Hughes TJR (eds) Encyclopedia of computational mechanics, vol 1. Wiley, West Sussex, England

Bartholdi JJ III, Gue KR (2004) The best shape for a crossdock. Transp Sci 38(2):235–244. DOI:10.1287/trsc.1030.0077

Bejan A (2000) Shape and structure, from engineering to nature. Cambridge University Press, Cambridge, UK

Bejan A, Ledezma GA (1998) Streets tree networks and urban growth: optimal geometry for quickest access between a finite-size volume and one point. Physica A 255(1–2):211–217. DOI:10.1016/S0378-4371(98)00085-5

Bendsøe MP, Sigmund O (1999) Material interpolation schemes in topology optimization. Arch Appl Mech 69(9–10):635–654. DOI:10.1007/s004190050248

Bendsøe MP, Sigmund O (2004) Topology optimization—theory, methods, and applications. Springer, Berlin Heidelberg New York

Borrvall T, Petersson J (2003) Topology optimization of fluids in Stokes flow. Int J Numer Methods Fluids 41:77–107. DOI:10.1002/fld.426

Craig KJ, de Kock DJ, Snyman JA (2001) Minimizing the effect of automotive pollution in urban geometry using mathematical optimization. Atmos Environ 35:579–587. DOI:10.1016/S1352-2310(00)00307-1

Chalot FL (2004) Industrial aerodynamics. In: Stein E, Borst R, Hughes TJR (eds) Encyclopedia of computational mechanics, vol 3. Wiley, West Sussex, England

Choi KK, Kim N-H (2005) Structural sensitivity analysis and optimization, 1 and 2. Springer, Berlin Heidelberg New York

Cockburn B, Karniadakis GE, Shu C-W (1999) Discontinuous Galerkin methods: theory, computation and applications. Springer, Berlin Heidelberg New York

Diaz AR, Benard A (2003) Topology optimization of heat-resistant structures. Proc ASME Des Eng Tech Conf 2A:633–639

Donoso A, Sigmund O (2004) Topology optimization of multiple physics probelms modelled by Poisson's equation. Latin Am J Solid Struct 1:169–184

Evgrafov A (2004) Topology optimization of slightly incompressible fluids. Ph.D. thesis: Approximation of topology optimization problems using sizing optimization problems, Department of Mathematics, Chalmers University of Technology, Göteborg, Sweden, pp 55–81. ISBN 91-7291-466-1

Gersborg-Hansen A, Sigmund O, Haber RB (2005a) Topology optimization of channel flow problems. Struct Multidiscipl Optim 30(3):181–192. DOI:10.1007/s00158-004-0508-7

Gersborg-Hansen A, Bendsøe MP, Sigmund O (2005b) Topology optimization using the finite volume method. In: Proceedings of the 6th world congress of structural and multidisciplinary optimization, Rio de Janeiro, 2005

Guillaume P, Idris KS (2005) Topological sensitivity and shape optimization for the stokes equations. SIAM J Control Optim 43(1):1–31. DOI:10.1137/S0363012902411210

Habbal A, Petersson J, Thellner M (2004) Multidisciplinary topology optimization solved as a Nash game. Int J Numer Methods Eng 61(7):949–963. DOI:10.1002/nme.1093

Hashin Z (1983) Analysis of composite-materials—a survey. J Appl Mech 50(3):481–505

Hashin Z, Shtrikman S (1962) A variational approach to the theory of the effective magnetic permeability of multiphase materials. J Appl Phys 33(10):3125–3131

Hovedstadens Udviklingsråd (2003) Trafikplan 2003 (in Danish). Available at www.hur.dk. ISBN 87-7971-110-3

Jenny P, Lee SH, Tchelepi HA (2004) Adaptive multiscale finite-volume method for multiphase flow and transport in porous media. Multiscale Model Simul 3(1):50–64. DOI:10.1137/030600795

Jha MK, Schonfeld P (2004) A highway alignment optimization model using geographic information systems. Transp Res Part A 38:455–481. DOI:10.1016/j.tra.2004.04.001

Jong JC, Schonfeld P (2003) An evolutionary model for simultaneously optimizing three-dimensional highway alignments. Transp Res Part B 37:107–128. DOI:10.1016/S0191-2615(01)00047-9

Klarbring A, Petersson J, Torstenfelt B, Karlsson M (2003) Topology optimization of flow networks. Comput Methods Appl Mech Eng 192(35–36):3909–3932. DOI:10.1016/S0045-7825(03)00393-1

Lesaint P, Raviart P-A (1974) On a finite element method for solving the neutron transport equation. In: de Boor C (ed) Mathematical aspects of finite elements in partial differential equations. Academic, New York

Li Q, Steven GP, Xie YM, Querin OM (2004) Evolutionary topology optimization for temperature reduction of heat conducting fields. Int J Heat Mass Transfer 47:5071–5083. DOI:10.1016/j.ijheatmasstransfer.2004.06.010

Mohammadi B, Pironneau O (2004) Shape optimization in fluid mechanics. Annu Rev Fluid Mech 36:255–279. DOI:10.1146/annurev.fluid.36.050802.121926

Olesen LO, Okkels F, Bruus H (2005) A high-level programming—language implementation of topology optimization applied to steady-state Navier–Stokes flow. Int J Numer Methods Eng. DOI:10.1002/nme.1468

Patankar SV (1980) Numerical heat transfer and fluid flow. Hemisphere, New York

Pedersen NL (2004) On optimization of bio-probes. Int J Numer Methods Eng 61:791–806. DOI:10.1002/nme.1026

Sigmund O (2001a) A 99 line topology optimization code written in MATLAB. Struct Multidiscipl Optim 21:120–127 (MATLAB code available online at: www.topopt.dtu.dk). DOI:10.1007/s001580050176

Sigmund O (2001b) Design of multiphysics actuators using topology optimization—Part I: one-material structures. Comput Methods Appl Mech Eng 190(49–50):6577–6604. DOI:10.1016/S0045-7825(01)00251-1

Sigmund O (2001c) Design of multiphysics actuators using topology optimization—Part II: two-material structures. Comput Mehtods Appl Mech Eng 190(49–50):6605–6627. DOI:10.1016/S0045-7825(01)00252-3

Sigmund O, Gersborg-Hansen A, Haber RB (2003) Topology optimization for multiphysics problems: a future FEMLAB application? In: Gregersen L (ed) Nordic Matlab conference (held in Copenhagen). Comsol, Søborg, Denmark, pp 237–242

Squire W, Trapp G (1998) Using complex variables to estimate derivatives of real functions. SIAM Rev 40(1):110–112. DOI:10.1137/S003614459631241X

Stolpe M, Svanberg K (2001) An alternative interpolation scheme for minimum compliance topology optimization. Struct Multidiscipl Optim 22(2):116–124. DOI:10.1007/s001580100129

Svanberg K (1987) The method of moving asymptotes—a new method for structural optimization. Int J Numer Methods Eng 24:359–373

Svanberg K (2002) A class of globally convergent optimization methods based on conservative convex separable approximations. SIAM J Optim 12(2):555–573. DOI:10.1137/S1052623499362822

Thellner M (2005) Topology optimization of convection–diffusion problems. Ph.D. thesis: Multi-parameter topology optimization in continuum mechanics. Linköping Studies in Science and Technology, Dissertations no. 934, pp 71–87. ISBN 91-85297-71-2

Torquato S, Gibiansky LV et al (1998) Effective mechanical and transport properties of cellular solids. Int J Mech Sci 40(1):71–82. DOI:10.1016/S0020-7403(97)00031-3

van Keulen F, Haftka RT, Kim NH (2005) Review of options for structural design sensitivity analysis. Part 1: linear systems. Comput Methods Appl Mech Eng 194(30–33):3213–3243. DOI:10.1016/j.cma.2005.02.002

Versteeg HK, Malalasekera W (1995) An introduction to computational fluid dynamics: the finite volume method. Longman Scientific & Technica, London

Vos JB et al (2002) Navier–Stokes solvers in European aircraft design. Prog Aerosp Sci 38:601–697. DOI:10.1016/S0376-0421(02)00050-7